

Damping of phase-mixed slow magneto-acoustic waves: Real or apparent?

Y. Voitenko¹, J. Andries^{1,*}, P. D. Copil¹, and M. Goossens¹

Centrum voor Plasma-astrofysica, K. U. Leuven, Celestijnenlaan 200B, 3001 Leuven, Belgium
e-mail: jesse.andries@wis.kuleuven.ac.be

Received 16 December 2004 / Accepted 29 May 2005

Abstract. The propagation of slow magnetoacoustic waves along a multithreaded coronal loop is modelled analytically by means of a ray tracing method. It is shown how cross field gradients build up due to phase mixing. The cross field gradients can enhance shear viscosity so that it dominates over compressive viscosity. Nevertheless the short dissipation distances ($\sim 10^7$ m) observed for slow waves in coronal loops require very small cross field length scales which imply a filamentary structure on scales at least three orders of magnitude below the current detection limit of TRACE and close to the limit where magnetohydrodynamic (MHD) theory breaks down. The observed dissipation distances can alternatively be explained by phase mixing in its ideal regime, where the apparent damping is due to the spatial integration of the phase mixed amplitudes by the observation.

Key words. Sun: corona – Sun: magnetic fields – Sun: oscillations – plasmas – waves

1. Introduction

Slow magnetoacoustic waves, are observed propagating upward along coronal loops by SOHO/CDS and TRACE (e.g. De Moortel et al. 2004; Marsh et al. 2003, and references therein). The short damping distances of these waves, $L_d \lesssim 10^7$ m, have not yet been explained adequately in terms of known mechanisms. In this Letter we want to address the interpretation of the observed damping in terms of phase mixing of slow waves. The process of phase mixing was first studied in the coronal environment for Alfvén waves by Heyvaerts & Priest (1983). The basic idea is that sufficiently short dissipative length-scales can be created in the cross-field direction due to the fact that the perturbations travel at different phase speeds along neighboring field lines. Since slow waves, like Alfvén waves, are very anisotropic and propagate mainly along the magnetic field lines, the consideration of a phase mixing process for slow waves is an obvious step. However, the phase mixing of slow mode waves has only recently been studied by De Moortel et al. (2004), in a plasma with a smooth density profile.

This Letter focusses on the following three points.

Firstly, there is increasing evidence that coronal loops have complex internal structure and consist of many thin strands (Aschwanden et al. 2000; Testa et al. 2002). Robbrecht et al. (2001) noted that the waves seem to propagate at different speeds when observed in different temperatures and have related that finding to a possible subresolution internal structure

of the loops. This implies that the description of a phase mixing process should be considered on a subresolution scale.

Secondly, the use of isotropic viscous damping (as used in previous studies) can by no means be justified in the corona, where $\Omega_p \tau_p = 10^4 \div 10^5$ (Ω_p is the proton cyclotron frequency, τ_p is the proton collision time). In this Letter we therefore start from the Braginskii coefficients (Braginskii 1965) and the proper values for shear and compressional viscosity.

Thirdly, we point out that it may be sufficient to consider the phase mixing process in its ideal regime, as the waves are always observed in an integrated sense (due to limited spatial resolution and line of sight integration). The weakening of the signal is then only apparent, just being due to the fact that the signals on different field lines are out of phase and cancel out by spatial integration during the observation. A similar suggestion of apparent damping has been made recently by Klimchuk et al. (2004), but they attribute the damping to a broadening of the wave front, while we rather attribute it to the annihilation of the phase mixed amplitudes through integration.

2. Damping due to phase mixing and anisotropic viscosity

The aim is to track the evolution of slow waves, excited at the footpoints of the magnetic field lines. The length scale of the transverse inhomogeneity of the equilibrium is L_\perp and the length scale of the field-aligned inhomogeneity of the equilibrium is L_\parallel . Both L_\perp and L_\parallel can vary over a wide range in the solar corona, but usually $L_\parallel \gg L_\perp$. Here we consider a perturbation with parallel and perpendicular wavelengths $\lambda_\parallel, \lambda_\perp$ which

* Postdoctoral Fellow of the National Fund for Scientific Research – Flanders, Belgium (F.W.O.-Vlaanderen).

are much shorter than the length-scales of the equilibrium inhomogeneity, $\lambda_{\parallel} \ll L_{\parallel}$, $\lambda_{\perp} \ll L_{\perp}$. The following analysis thus in principle describes only the developed phase of phase mixing. The initial stages of the phase mixing process where cross-field gradients evolve from an initially smooth perpendicular profile are not described here. In that respect the values for the damping lengths calculated below should be considered as lower limits. The numerical results by De Moortel et al. (2004) suggest that also the initial evolution is indeed accurately described by the propagation of local slow waves confined to the field lines and their coupling to other modes is weak in comparison to their observed damping. On the other hand, numerical simulations by Malara et al. (1996) have demonstrated that the oblique propagating Alfvén wave can be efficiently coupled to compressional modes when $\lambda_{\perp} \sim \lambda_{\parallel}$. However, in their simulations Malara et al. imposed periodicity along the direction of background magnetic field, which is quite different from those used in our model and in the simulations by De Moortel et al. (2004).

Given the above assumptions¹ and by use of a *local coordinate system* with z along the equilibrium magnetic field and x along the equilibrium cross-field gradient, the coupled viscous MHD equations for the field-aligned (v_z) and cross-field (v_x) components of the velocity perturbation are obtained by use of Braginskii's (Braginskii 1965) equations as:

$$\left(\frac{\partial^2}{\partial t^2} - V_s^2 \frac{\partial^2}{\partial z^2}\right)v_z - V_s^2 \frac{\partial^2}{\partial z \partial x} v_x - \frac{2}{3}v_0 \frac{\partial}{\partial t} \frac{\partial}{\partial z} \left(\frac{\partial}{\partial x} v_x - 2 \frac{\partial}{\partial z} v_z\right) + v_2 \frac{\partial}{\partial t} \frac{\partial^2}{\partial x^2} v_z \quad (1)$$

$$\left(\frac{\partial^2}{\partial t^2} - [V_s^2 + V_A^2] \frac{\partial^2}{\partial x^2} - V_A^2 \frac{\partial^2}{\partial z^2}\right)v_x - V_s^2 \frac{\partial^2}{\partial z \partial x} v_z = \frac{1}{3}v_0 \frac{\partial}{\partial t} \left(\frac{\partial^2}{\partial x^2} v_x - 2 \frac{\partial^2}{\partial z \partial x} v_z\right) + v_1 \frac{\partial}{\partial t} \frac{\partial^2}{\partial x^2} v_x \quad (2)$$

with V_s and V_A the sound and Alfvén speed as usual. These equations differ from those used by De Moortel et al. (2004) only by the dissipative terms. Here the specific viscosity coefficients correspond to the Braginskii coefficients: $v_0 = 0.96\tau_p k_B T_p / m_p$; $v_2 = (\Omega_p \tau_p)^{-2} v_0$; $v_1 = v_2/4$ where $\rho_0 = n_0 m_p$ is the mass density and τ_p the proton collision time.

Since we are assuming $\lambda_{\parallel} \ll L_{\parallel}$ and $\lambda_{\perp} \ll L_{\perp}$ we can consider the evolution of the perturbation by means of a ray tracing method using the WKB-ansatz:

$$A = A_0 \times \exp\left(-i\omega t + i \int \mathbf{k} \cdot d\mathbf{r} + \int \gamma dt\right). \quad (3)$$

The wave vector \mathbf{k} and the increment γ have to be calculated from the *local dispersion relation*, and the integration is along the path of the wave propagation which is determined by the ray equations for the wave vector \mathbf{k} and position \mathbf{r} :

$$\frac{d\mathbf{k}}{dt} = -\frac{\partial \omega}{\partial \mathbf{r}}, \quad \frac{d\mathbf{r}}{dt} = \frac{\partial \omega}{\partial \mathbf{k}}. \quad (4)$$

¹ The assumption $\lambda_{\perp} \ll L_{\perp}$ is not entirely necessary at this point but we will have to adopt it at a later stage anyway.

The effects of the plasma inhomogeneity on the waves are due to the spatial dependence of the plasma parameters along the path of the wave propagation. The local dispersion relation is obtained from Eqs. (1)–(2) by substituting $\partial/\partial t \rightarrow -i\omega + \gamma$, $\partial/\partial x \rightarrow ik_x$, $\partial/\partial z \rightarrow ik_z$. When the damping rate is small the slow wave frequency can be obtained as an expansion in $\beta = V_s^2/V_A^2$:

$$\omega^2 = (1 - \beta + O(\beta^2)) k_z^2 V_s^2. \quad (5)$$

According to Eq. (4) slow waves propagate almost purely along the magnetic field in a low β plasma. Equation (4) furthermore yields:

$$k_{\perp, \parallel} = k_{\perp, \parallel 0} \pm \frac{\omega t}{L_{\perp, \parallel}} = k_{\perp, \parallel 0} \pm \frac{k_{\parallel} V_s t}{L_{\perp, \parallel}} = k_{\perp, \parallel 0} \pm \frac{z}{L_{\perp, \parallel}} k_{\parallel},$$

where the integration is performed under the assumption that $z \ll L_{\parallel}$ which is true for the observed waves. Although the inhomogeneity along the magnetic field lines may slowly change the parallel length scales of the perturbation, k_{\parallel} cannot change significantly for the observed travelling distances $z \ll L_{\parallel}$, and can thus be assumed constant over the observed travelling distance. Perpendicular length scales on the contrary decrease rather quickly since $z \gg L_{\perp}$ when the filamentary structure is taken into account. After a rather short initial stage $k_{\perp 0}$ can be ignored and the perpendicular length scales keep on decreasing very fast as $k_{\perp} \approx k_{\parallel} (z/L_{\perp})$.

The damping rate can furthermore be computed to be:

$$\gamma = -\frac{1}{2} \left(\frac{4}{3} v_0 k_z^2 + v_2 k_x^2 \right) = -\frac{1}{2} v_0 \left(\frac{4}{3} k_z^2 + (\Omega_p \tau_p)^{-2} k_x^2 \right).$$

The first term in this expression is due to compressional viscosity while the second is due to shear viscosity. As we have argued, the cross-field gradients quickly dominate and thus the shear viscosity starts dominating after a distance $z/L_{\perp} > 2/\sqrt{3}\Omega_p \tau_p \approx 2 \times 10^4$. For the decrease of the wave amplitude along the ray path we obtain:

$$A_s = A_{s0} \times \exp\left(-\frac{z}{z_{c-v}} - \frac{z^3}{z_{s-v}^3}\right)$$

where z_{c-v} and z_{s-v} are the typical dissipation distance due to compressional viscosity and to shear viscosity respectively:

$$z_{c-v} = \frac{3}{2} \frac{V_s}{v_0 k_z^2}, \quad z_{s-v} = \sqrt[3]{\frac{6V_s L_{\perp}^2 (\Omega_p \tau_p)^2}{v_0 k_z^2}}. \quad (6)$$

As we see, the Heyvaerts-Priest-like decay of the Alfvén wave amplitude with height, $\exp(-z^3)$, is also obtained for dissipation of slow magneto-acoustic waves by shear viscosity. Moreover, the damping distance by shear viscosity, contrary to that for compressive viscosity, depends on the cross field length scales and could thus be brought down considerably by accounting for the observed filamentary structure.

Typical values for the phase speed and period are 1.2×10^5 m/s and 300 s (e.g. De Moortel et al. 2002). With these numbers the slow wave dispersion relation yields a parallel wave length of around 3.6×10^7 m. It must be noted that this is

longer than the typical observation length of $8.9 \pm 4.4 \times 10^6$ m. This is indeed in accordance with the fact that hardly half of a wavelength seems to be visible in the running difference images (see e.g. the running difference image in Marsh et al. 2003). With a value of $v_0 = 1.4 \times 10^9$ m²/s those numbers yield a compressional damping length of $z_{c-v} \approx 4.2 \times 10^9$ m, which is clearly more than two orders of magnitude too large to explain the observed damping lengths of $\approx 10^7$ m. If phase mixing is expected to enhance the cross field gradients sufficiently fast so that shear viscous damping becomes more effective than the compressional damping (which we just found inefficient), then we at least need $L_{\perp} < \frac{1}{2} (\Omega_p \tau_p)^{-1} z_{c-v} \approx 1.2$ km, where we have used $\Omega_p = 10^5$ s⁻¹ and $\tau_p = 0.17$ s. More precisely, the explanation of the observed damping lengths of the order of $\approx 10^7$ m requires cross field equilibrium length scales shorter than:

$$L_{\perp} < \frac{1}{\Omega_p \tau_p} \sqrt{\frac{v_0 k_z^2 z_{\text{obs}}^3}{6V_s}} \approx 14 \text{ m.}$$

If the density contrast of the threads is of the order of 2, then this also represents the required dimension of the strands. For larger density contrasts between threads, the widths of the threads may well be up to 100 m. While this is at least three orders of magnitude below the current detection limit of TRACE, it is only one order of magnitude below the finest filamentary scales found by Woo & Habbal (1997). The value of 14 m is still longer than the proton (and electron) Larmour radius, $\rho_p = 0.5$ m, but it is only one order of magnitude larger the critical length scale of one meter at which the non-uniformity still can be sustained. Therefore, even if such small length scales are present in the coronal loops we suggest it is unlikely that the observed damping lengths can be explained with a combined mechanism of phase mixing and shear viscous damping in the context of magnetohydrodynamics.

3. Apparent damping

The point we address here is whether the observed disappearance of propagating waves has anything to do with real dissipation or rather is just apparent. Therefore, let us calculate the observed signal of phase-mixed slow waves in the ideal regime. It can be anticipated that when waves within one pixel get out of phase, the integrated signal is weakened.

The linear part of the excess emission measure at a particular pixel (of size L_p) due to the linear density perturbations n_1 on the equilibrium density n_0 is:

$$EM_1 = EM - EM_0 = L_p^{-1} \int_{L_p} G 2n_0 n_1 dx$$

where G indicates the temperature filter of the device so that only emission from plasma at filter sensitive temperatures is picked up. In order to keep the mathematical analysis as simple as possible we use a highly simplified response function, namely a hat function picking up only signals from plasma at temperatures between $(1 - w/2)T_0$ and $(1 + w/2)T_0$, where w is thus a measure of the filter width. Due to the temperature inhomogeneity $T(x)/T_0 = 1 + x/L_{\perp}$, signals are picked up from

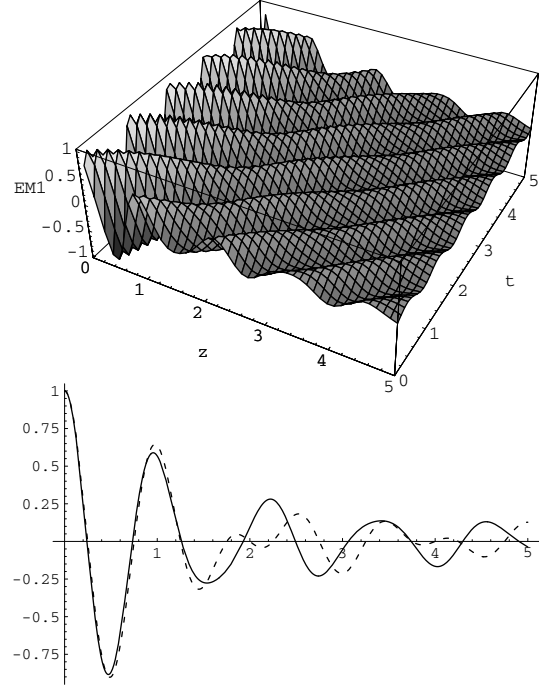


Fig. 1. The normalized linear part of the excess emission measure integrated over one pixel **a)** as a function of longitudinal distance z and time t normalized with respect to the central longitudinal wavelength and the period respectively. **b)** as a function of the longitudinal distance z for time $t = 0$. The dashed line is the analytic approximation to the integral.

strands with a width of $L_G = wL_{\perp}$. Now let us assume that these strands are below pixel resolution $L_G < L_p$ then:

$$EM_1 = 2fn_0 \frac{1}{L_G} \int_{-L_G/2}^{L_G/2} n_1 dx$$

where $f = N \times L_G/L_p$ is the filling factor with N the number of strands in the pixel. We consider n_1 as the signal of phase mixed slow waves travelling with different phase speeds and thus different parallel wave lengths on different field lines:

$$n_1(x, z, t) = n_{10} \cos \left[2\pi \frac{1}{\sqrt{1+x/L_{\perp}}} \frac{z}{\lambda_{\parallel 0}} - 2\pi \frac{t}{\tau} \right].$$

We thus obtain:

$$EM_1 = 2fn_0 n_{10} \frac{1}{w} \int_{-w/2}^{w/2} \cos \left[2\pi \frac{1}{\sqrt{1+y}} \frac{z}{\lambda_{\parallel 0}} - 2\pi \frac{t}{\tau} \right] dy. \quad (7)$$

The line-of-sight integration gives the same result provided there are several strands along the line of sight. If $w \ll 1$, $1/\sqrt{1+y}$ can be expanded and the integral worked out to be:

$$EM_1 = 2fn_0 n_{10} \frac{2\lambda_{\parallel 0}}{\pi zw} \sin \left[\frac{\pi zw}{2\lambda_{\parallel 0}} \right] \cos \left[2\pi \frac{z}{\lambda_{\parallel 0}} - 2\pi \frac{t}{\tau} \right].$$

In reality, however, w is not small but of order unity for the TRACE Å171 bandpass (see Bentley et al. 2000) and thus integral (7) needs to be calculated numerically. Figure 1a shows the result for $w = 1$ as a function of z and t where distances and time are normalized with respect to $\lambda_{\parallel 0}$ and τ . Figure 1b shows

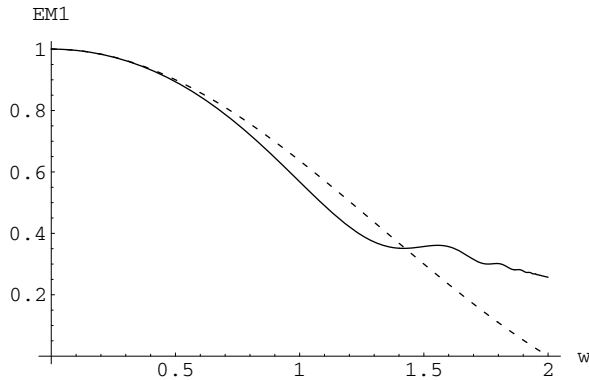


Fig. 2. The rate of weakening of the signal as a function of the filter width w . The dashed line is obtained with the analytic approximation and is thus only valid for small w .

only the z dependence and the dashed line corresponds to the analytic result which appears to behave well up to about one wavelength (despite the violation of condition $w \ll 1$). As can be seen, the amplitude of the signal decreases almost by half of its value in about one wavelength. Clearly a narrower filter would result in less weakening of the signal while a broader filter yields faster weakening of the signal. Therefore, Fig. 2 shows the strength of the signal after one wavelength as a function of w . Clearly, we should conclude that substantial weakening of the signal can occur in one wavelength if the width of the filter is of order unity or higher.

The above results are obtained using only the perpendicular variation of temperature (phase speed) and a simplified filter function. While more realistic calculations might change these results slightly, we believe that the present calculations show the basic ingredients of the process and have identified the width of the temperature filter as a crucial parameter in the problem.

4. Conclusions and discussion

We have solved the MHD equations analytically by means of a ray tracing method and have thereby shown that phase mixing of slow waves may reduce the damping length by shear viscosity below the damping length by compressional viscosity. However, to explain the very small damping lengths for the

observed slow waves in coronal loops, extremely small equilibrium cross field length scales are required which are at least 4 orders of magnitude below the current detection limit. Those length scales are also close to the length scales at which the MHD approximation breaks down. It thus seems unlikely that such a process is responsible for the fast damping of the observed slow waves in coronal loops unless the anomalous viscosity comes into play.

However, phase mixing need not be ruled out with respect to the fast damping of slow waves in coronal loops. Even in the ideal phase the spatially integrated signal weakens as the waves get out of phase. Our calculations show that the conditions for this apparent damping to be substantial is quite mild. The width of the temperature filter has to be of the order of the peak temperature and that temperature range has to be present on a sub-resolution scale (or, alternatively, within the line-of-sight integration distance).

Acknowledgements. The authors are thankful to Dr. De Moortel for introducing them to the subject of propagating slow waves in coronal loops. This work was supported by the FWO-Vlaanderen grants G.0335.98 and G.0178.03, by the Onderzoeksfonds K. U. Leuven grant OT/02/57, and by Intas grant 96-530.

References

- Aschwanden, M. J., Nightingale, R. W., & Alexander, D. 2000, *ApJ*, 541, 1059
- Bentley, R. D., Klein, K.-L., van Driel-Gesztelyi, L., et al. 2000, *Sol. Phys.*, 193, 227
- Braginskii, S. I. 1965, *Rev. Plas. Phys.*, 1, 205
- De Moortel, I., Ireland, J., Walsh, R. W., & Hood, A. W. 2002, *Sol. Phys.*, 209, 61
- De Moortel, I., Hood, A. W., Gerrard, C. L., & Brooks, S. J. 2004, *A&A*, 425, 741
- Heyvaerts, J., & Priest, E. R. 1983, *A&A*, 117, 220
- Klimchuk, J. A., Tanner, S. E., & de Moortel, I. 2004, *ApJ*, 616, 1232
- Malara, F., Primavera, L., & Veltri, P. 1996, *ApJ*, 459, 347
- Marsh, M. S., Walsh, R. W., De Moortel, I., & Ireland, J. 2003, *A&A*, 404, L37
- Robbrecht, E., Verwichte, E., Berghmans, D., et al. 2001, *A&A*, 370, 591
- Testa, P., Peres, G., Reale, F., & Orlando, S. 2002, *ApJ*, 580, 1159
- Woo, R., & Habbal, S. R. 1997, *ApJ*, 474, L139